

Large-Scale Atmospheric Circulation Characteristics as Evident from Ghost Balloon Data¹

GENE WOOLDRIDGE AND E. R. REITER

Dept. of Atmospheric Science, Colorado State University, Fort Collins

(Manuscript received 8 September 1969, in revised form 8 December 1969)

ABSTRACT

From GHOST balloon data obtained over the Southern Hemisphere at the 200-mb level, phase velocities of cyclone waves were found to vary between 6.3 and 9.2 degrees of longitude per day. Spectrum analysis of the relative velocities of balloon pairs, measured with respect to their common center of gravity, yielded a spectrum peak in the v component near frequencies of 1/52 hr, and a “-3” spectrum slope at higher frequencies. (The latter may be contaminated by a spline function smoothing technique.) Spectral densities in v were found to be slightly larger in summer than in winter, while densities in u were half as large in summer than in winter. Significantly stronger anisotropy of flow prevails at cyclone wavelengths in the Southern than the Northern Hemisphere, with the v perturbations exceeding the zonal flow perturbations. GHOST balloon cospectra yielded similar results of momentum transport as did data from the Northern Hemisphere.

Eulerian spectra of the v component over New Zealand agreed well with results from the Northern Hemisphere; spectral densities of the u component in the Southern Hemisphere, however, were approximately half of those found in the Northern Hemisphere (Washington, D. C.); the v spectra showed a peak at 1/14 day. Spectrum slopes of “-1” are indicated at higher frequencies. Eulerian cospectra permitted a preliminary estimate of meridional transports of zonal momentum.

A crude estimate of the relation between Eulerian and Lagrangian spectra yielded considerably different results for the Southern than for the Northern Hemisphere as did estimates of the coefficients of eddy diffusivity K_x and K_y .

1. Introduction

GHOST balloons launched from New Zealand during 1966 and 1967 and drifting at the 200-mb level provided the main data source of this investigation of Southern Hemisphere flow characteristics (Solot, 1968). In addition, rawinsonde data from Invercargill and Christchurch, New Zealand, and Kerguelen Island, were used in a comparison of Lagrangian and Eulerian spectra of atmospheric perturbation motions.

Extensive research on Southern Hemisphere disturbances has been reported recently by van Loon (1964, 1965) and Taljaard (1967). The new tool of the constant-density balloon is employed in the present study.

In the Northern Hemisphere, where data are more plentiful, spectrum analyses of perturbation motions in Lagrangian and Eulerian coordinate systems have been carried out by a number of authors (Chiu, 1960; Mantis, 1963; Kao and Bullock, 1964; Kao, 1965; Chiu and Crutcher, 1966; Kao and al-Gain, 1968; Vinnichenko and Dutton²; Vinnichenko³). The results

of these studies serve well for a preliminary comparison of Northern and Southern Hemisphere flow characteristics. These comparisons may be expanded as soon as more data from constant-density balloons and from rawinsonde stations become available and are processed.

The dispersion of atmospheric trace substances, either naturally or artificially generated, is strongly affected by the statistical characteristics of the flow patterns in the free atmosphere. The separation rate of “balloon pairs” serves as a crude indicator of the diffusive effects of planetary and cyclone scale motions.

2. GHOST balloons as quasi-Lagrangian tracers of wave motions

One of the tasks a global Lagrangian measurement system will have to fulfill is to properly identify standing and traveling planetary and cyclone waves. A serious problem exists in estimating wavelengths, phase speeds and amplitudes of those wave phenomena which travel at a speed comparable to the velocity of the balloon.

A simple experiment was conducted in order to estimate the usefulness of GHOST balloons in identifying large-scale atmospheric wave phenomena. The wind directions as reported in the data books (Solot, 1968)

sphere—1 second to 5 years. Paper presented at Intern. Symp. on Spectra of Meteorological Variables, Stockholm, Sweden, June 1969.

¹ The research reported in this paper was supported by the U. S. Atomic Energy Commission under Contract AT(11-1)-1340.

² Vinnichenko, N. K., and J. A. Dutton, 1969: Empirical studies of atmospheric structure and spectra in the free atmosphere. Paper presented at Intern. Symp. on Spectra of Meteorological Variables, Stockholm, Sweden, June 1969.

³ Vinnichenko, N. K., 1969: The kinetic energy in the free atmo-

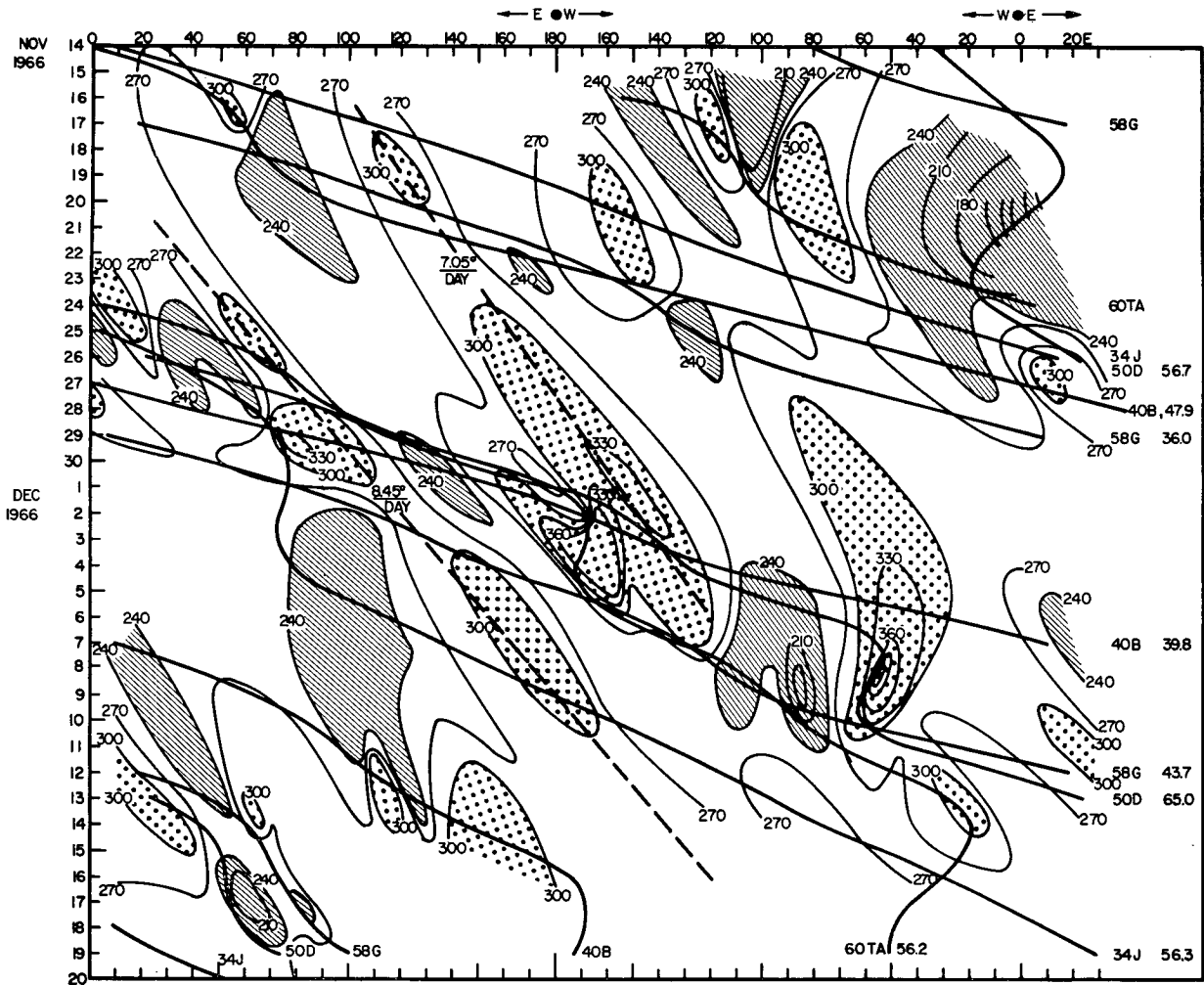


FIG. 1. GHOST balloon direction of motion as a function of longitude and time for Southern Hemisphere summer 1966. Slanted hatching indicates directions $< 240^\circ$, dotted areas indicate directions $> 300^\circ$. Slanted solid lines are balloon paths (balloon numbers and average latitudes at right margin). Slanted dashed lines are phase velocities.

were analyzed in time-longitude diagrams, with a certain degree of subjectivity on account of sparse data and varying geographic latitudes at which the balloons were found from day to day. Results for November–December 1966 and June–July 1966 obtained at 200 mb are shown in Figs. 1 and 2.

Several trough-ridge patterns may be identified in both diagrams, moving eastward with the speeds ranging between 6.3 and 9.2 degrees of latitude per day. From the data sample presented here no significant changes in the phase speed of short cyclone waves between summer and winter could be detected. This conforms to van Loon's (1965) findings for the 500-mb level, which actually revealed slightly higher average phase speeds during the Southern Hemisphere summer than during winter (Fig. 3). Average Northern Hemisphere phase speeds of short cyclone waves on the 700-mb surface, according to Namias (1947), are 8.0 degrees of longitude per day for summer and 11.8° per day for winter (see also Petterssen, 1956; Reiter, 1958).

Van Loon (1965) attributes the higher phase velocity C found during summer to the stronger zonal current u (see Fig. 4) and to the shorter wavelengths L that prevail during this season, in accordance with the Rossby wave equation

$$C = u - \frac{\beta L^2}{(4\pi^2)}, \tag{1}$$

where $\beta = \partial f / \partial y$ is the Rossby parameter and f the Coriolis parameter. Some inaccuracies from (1) may result due to divergence fields at 200 mb. The average balloon drift velocities computed from Figs. 1 and 2 indicate a different seasonal variation of u . Taking only those balloon trajectories which traverse the whole hemisphere, one obtains an average speed of 27.4 degrees of longitude per day for summer (7 trajectories), and 29.5° per day for winter (8 trajectories). The inclusion of the short trajectory pieces in the lower left of Fig. 1 (summer case) would tend to increase this

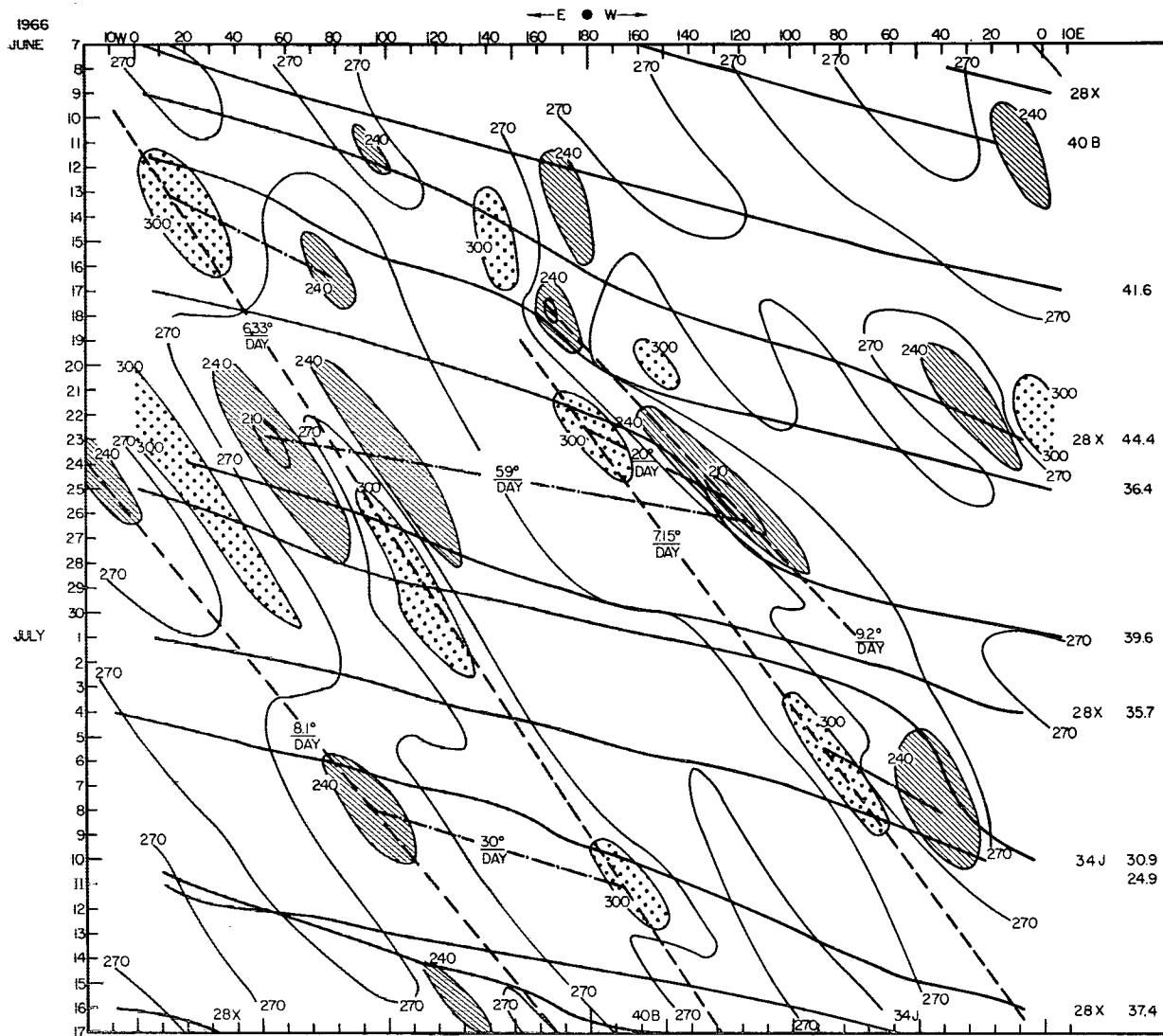


FIG. 2. Same as Fig. 1 except for winter, and with the addition of slanted dot-dashed lines for group velocities.

seasonal difference in drift velocities. The average latitudes of balloon trajectories considered in the above values of mean drift velocities are 49.3° for summer and 36.4° for winter. These latitudes lie close to the mean jet-stream positions found by van Loon and given in Fig. 4. Apparently the balloons entered the jet stream and stayed in its influence region, with the exception of the short trajectory pieces shown in Fig. 1 and not used for the above mean speed estimates.

The reasons for the discrepancies between the seasonal wind speed variations evident from the GHOST data and those from van Loon's statistics might lie in the fact that the latter pertain to the 500-mb level, whereas the GHOST data considered here are from the 200-mb level. Fig. 4 seems to indicate that during the winter season two jet-stream bands prevail in the Southern Hemisphere (see also van Loon, 1964). The band closest to the equator, in which the balloons

drifted during the winter experiment, probably is characteristic of the subtropical jet stream with its core close to 200 mb (Hutchings, 1950; Gibbs, 1952; Jenkinson, 1955; Radok and Clarke, 1958). During the summer experiment the 200-mb balloons most likely drifted above the level of maximum wind.

From Eulerian data, van Loon (1965) was able to identify events indicating horizontal energy dispersion of cyclone waves with group velocity C_g according to

$$C_g = u + \frac{\beta L^2}{(4\pi^2)} \quad (2)$$

Computed values, according to van Loon, for C_g were 30 degrees of longitude per day in winter (similar to Northern Hemisphere values; see Reiter, 1958) and 36° per day in summer. Observed values were 33° and 28° per day, respectively.

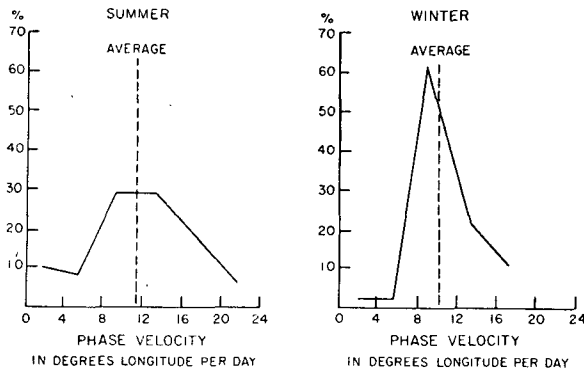


FIG. 3. Frequency distributions in per cent of the speeds of movements of troughs at the 500-mb level during the southern winter of 1957 and summer of 1958. Units are degrees of longitude per day (after van Loon, 1965).

The GHOST data in Figs. 1 and 2 reveal only a few events that might be construed as group velocity effects. Apparently, the mean drift velocities of the balloons at 200 mb are too close to the expected group velocities to allow reliable identification of energy dispersion in a Lagrangian coordinate system.

3. Lagrangian and Eulerian spectra and cospectra in the Southern Hemisphere

a. GHOST balloon spectra

The 200-mb GHOST balloons used in this study were released from Christchurch, New Zealand, and tracked by means of sun angle data derived from GHOST observations. Smoothing was performed over each balloon data population by means of two spline interpolation functions, one for latitude and one for longitude. Hourly latitude and longitude position values taken from the smoothed track constituted the data for analysis.

The balloon data used were derived from pairs of balloons which arrived at common longitudes at various latitude separations. Thirteen pairs of balloons were chosen for the summer data population (November

1966–March 1967); seven pairs were selected for the winter data population (May–August 1966). Hourly locations for each balloon of each pair for 48 hr before and 48 hr following arrival at the same longitude provided 97 latitude and longitude values for each balloon.

The hourly location of the common center of gravity for each pair was computed, and the velocity for each balloon relative to this common center of gravity calculated. The zonal and the meridional components of the relative separation velocities were combined into data series for both summer and winter. The spectral densities of the zonal and the meridional components and the u - v cospectral densities for summer and winter were computed by the standard Blackman and Tukey (1958) technique on a CDC 6400 computer.

The geographic latitudes of the balloons for the winter cases ranged from 10–65S with a mean of 41S; for the summer cases from 35–76S with a mean latitude of 62S. This seasonal shift of balloon tracks is similar to the one described in Section 2.

The spectra for the summer zonal and meridional components of relative separation velocities of the GHOST balloons are shown in Fig. 5. The spectral density of the zonal component decreases with increasing frequency k with an average power law of k^{-3} . The spectral density of the meridional component increases to a maximum at a frequency of about 1/52 hr and then decreases with increasing frequency. The winter spectral densities of the zonal and meridional components of relative velocities (Fig. 6) exhibit a similar peak of meridional spectral density at about 1/52 hr with the zonal density decreasing again, approximately following a k^{-3} distribution.

The spectral densities of the summer meridional component is slightly larger than that of the winter meridional component, while that of the summer zonal component is only about one-half that of the winter values. This is in approximate agreement with van Loon's (1965) analysis of 500-mb meridional flow in the Southern Hemisphere during the IGY. Van Loon found that while meridional flow increased from summer to winter north of 46S,

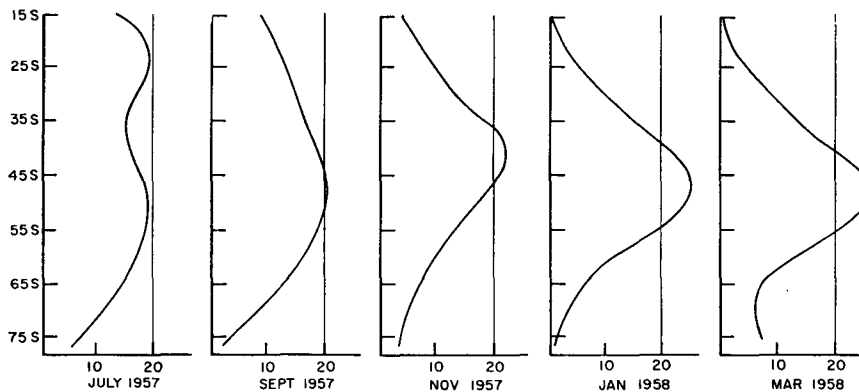


FIG. 4. Time section of monthly average zonal geostrophic wind at the 500-mb level for July 1957 to March 1958. Units are m sec^{-1} (after van Loon, 1965).

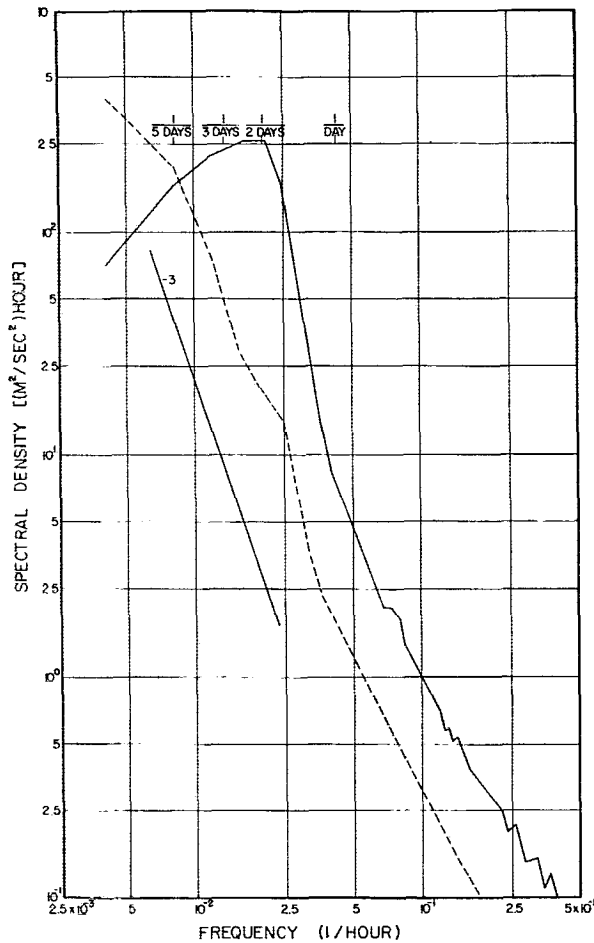


FIG. 5. Spectra of summer zonal (dashed line) and meridional (solid line) components of GHOST balloon relative separation velocities. The -3 line indicates the slope of a k^{-3} exponential function.

it decreases slightly south of 46S, in contrast to the Northern Hemisphere where the meridional flow decreased in summer at all latitudes.

The 52-hr period of meridional perturbation is very close to the characteristic 54-hr period computed by Angell (1960) for the 300-mb meridional wind in the Northern Hemisphere. Angell's analysis was based on transosonde flights originating over Japan and traveling eastward over North America. At the peak of his meridional spectral density the ratio of meridional to zonal spectral density was about 3 to 1.

A spectral analysis of zonal and meridional components of relative separation velocities at 200 mb in the Northern Hemisphere (Kao and al-Gain, 1968) showed a peak at about $\frac{1}{3}$ day in the meridional direction and a slope of about k^{-3} of the spectral density of the zonal component. The spectra were based on isobaric stream-function trajectories originating from a "cluster" of points off the northwestern United States. The ratio of the spectral densities derived from this study

was about 3 to 1 for meridional to zonal components of the relative velocities at the peak frequency.

The GHOST balloon meridional to zonal ratio, however, is about 10 to 1 at the same perturbation frequency of 1/52 hr. This would mean that a stronger anisotropy prevails at, or slightly above, jet-stream level in the Southern Hemisphere at this perturbation frequency than in the Northern Hemisphere.

The "velocity normalization" of the spectra calculated by Kao and al-Gain probably decreased the ratio of meridional to zonal velocity spectral densities. When the same normalization procedure is applied to the spectral densities of the separation velocity components for the GHOST balloon pairs, the ratio between meridional and zonal spectral densities still remains at 8 to 1 at the "peak" frequency of 1/52 hr. The anisotropy of the large-scale circulation of the Southern Hemisphere is thus quite significant, even if the spectra are normalized. The circulation of the Southern Hemisphere in the domain of cyclone waves is even more "meridional" than that of the Northern Hemisphere.

The greater variance in the meridional component of the relative separation velocities at the scale of

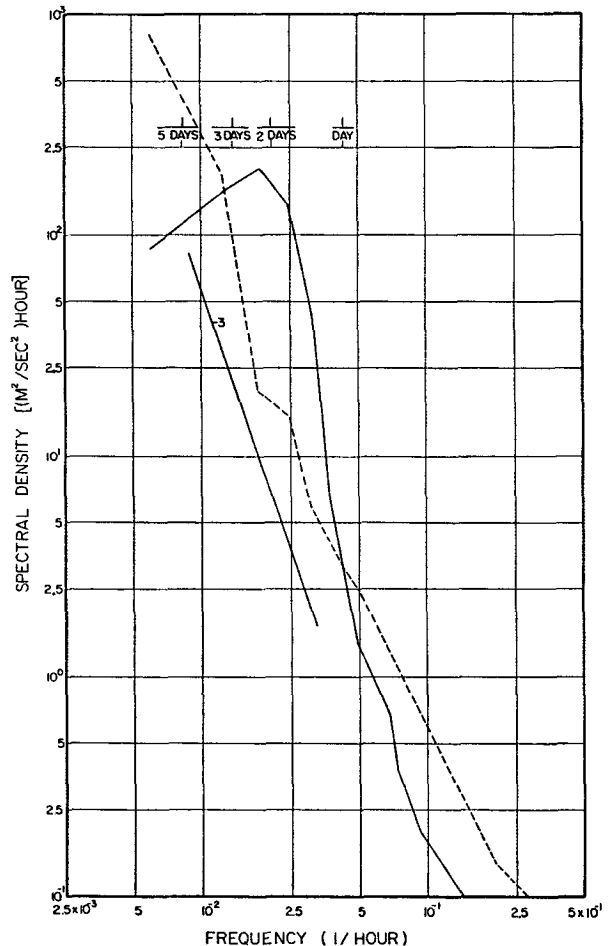


FIG. 6. Same as Fig. 5 except for winter.

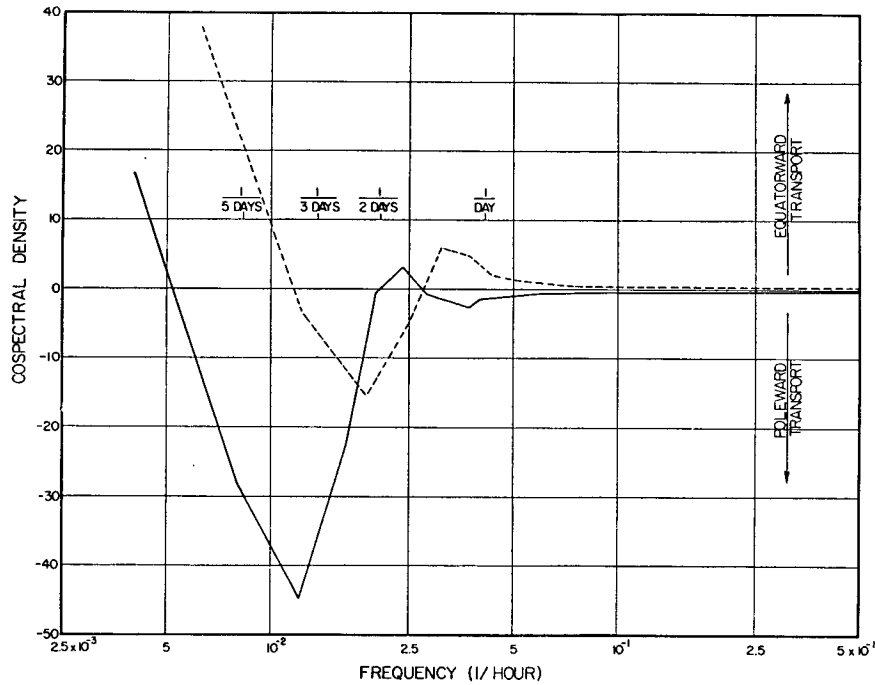


FIG. 7. Cospectra of zonal and meridional components of GHOST balloon relative velocities for summer (solid line) and winter (dashed line). Positive ordinate values indicate equatorward transport of relative angular momentum; negative values indicate poleward transport.

cyclone waves found in the Southern Hemisphere may be partially explained by two factors: 1) a higher frequency of low pressure centers, and 2) stronger meridional mass transport were measured by van Loon (1965) and Taljaard (1967) in the Southern Hemisphere, using IGY data, as compared to the Northern Hemisphere. Taljaard found a region of frequent low pressure activity along a belt from southern New Zealand to the Chilean Coast with a maximum frequency near 62S in summer.

A cursory examination of video satellite photographs was performed to determine the relative frequency of clearly defined synoptic-scale cloud vortices indicative of large middle latitude troughs. At the same time, the stretching of the vortices was measured by the ratio of the latitudinal to longitudinal extent of the pronounced cloud patterns, $r = \Delta\phi/\Delta\lambda$. A total of 167 vortices for the 30 days of the Southern Hemisphere summer month of December 1968 and 141 vortices for the Northern Hemisphere summer month of June 1968 revealed a small but significant difference in latitudinal vortex stretching in the two hemispheres. The average difference may be expressed by

$$\frac{r_{N.H.}}{r_{S.H.}} = \frac{6}{7}. \quad (3)$$

The zonal and meridional spectra for winter and summer in the Southern Hemisphere give indication of smoothing which results from application of spline functions to the GHOST balloon position data. High-

frequency contributions to the spectral densities appear to be suppressed in all cases. As an analogue to the application of spline function smoothing to GHOST balloon data, a test case was carried out on a randomly fluctuating radius of a circle. The varying radius values were run on a cubic spline program with a certain maximum allowable movement of point values. The radius values were repeated in a cyclic manner and subjected to the standard Blackman and Tukey spectral analysis before smoothing and again after smoothing. In the test case, the first one-fourth (18 out of a total of 72) of the wavenumbers was only slightly changed by the smoothing process. The next one-third of the wavenumbers was reduced in spectral density to $\sim 30\%$, and the remaining wavenumbers to $\sim 20\%$ compared to the raw data. This simple analogue emphasizes the fact that no interpretation should be made of the high-frequency portion of the GHOST balloon spectra, but that the low-frequency end is little changed by the smoothing interpolation process.

b. GHOST balloon cospectra

The $u-v$ cospectra for the winter and summer cases of the separation velocities of GHOST balloon pairs are shown in Fig. 7. The summer cospectrum indicates maximum poleward transport of momentum at a frequency of about $\frac{1}{4}$ day, in excellent agreement with that calculated by Kao and al-Gain (1968) for 200 mb in the Northern Hemisphere on an annual basis. The winter cospectrum, however, shows a much reduced poleward

transport at a frequency of about $\frac{1}{3}$ day, and increased equatorward transport at low frequencies. This shift may be due to the difference in the mean latitudes of the summer and winter GHOST balloon tracks or to the change in location of the jet stream with respect to the 200-mb level in summer and winter.

c. Eulerian wind spectra

As a basis for comparing synoptic-scale Southern Hemisphere Lagrangian and Eulerian spectra and Southern and Northern Hemisphere Eulerian spectra, one year of 200-mb daily wind data taken at 0000 GMT over Christchurch (43°29'S, 172°32'E) and Invercargill (46°25'S, 168°20'E), New Zealand, and Kerguelén Island (49°21'S, 70°13'E) were spectrally analyzed. The standard Blackman and Tukey method was employed to compute the spectra which are displayed in Figs. 8-10 for 1966.

The spectral densities of the meridional wind components for Christchurch (Fig. 8) and Invercargill (Fig. 9) increase with increasing frequency to a peak density at 1/14 day, and then decrease toward higher frequencies with a slope of approximately -1 on the log-log presentation. Kerguelén Island (Fig. 10) exhibits peak frequencies at 1/30 and at $\sim 1/10$ day, with a decrease of spectral densities toward higher frequencies approximating a -1 slope. Invercargill exhibits higher densities than Christchurch at frequencies $> 1/5$ day as might be expected since it is closer to the belt of high frequency of low pressure centers (van Loon, 1965). At lower frequencies the two New Zealand stations show similar spectra.

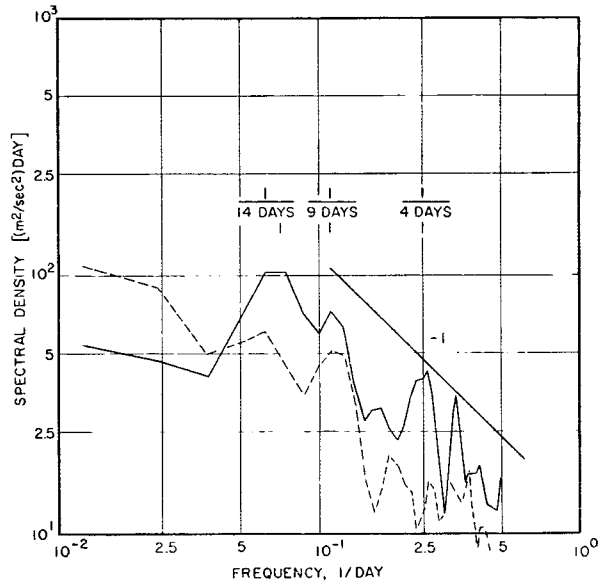


FIG. 9. Same as Fig. 8 except for Invercargill, New Zealand.

The slope of the log-log presentation of spectral density vs frequency agrees with that observed by Vinnichenko (*loc. cit.*) on the synoptic scale in the Northern Hemisphere. When values for the meridional component from Vinnichenko's smoothed curve of spectral densities are converted from $(\text{km}^2 \text{ day hr}^{-2} \text{ cycle}^{-1})$ to $(\text{m}^2 \text{ day sec}^{-2} \text{ rad}^{-1})$ used in this paper, quantitative agreement follows. The spectral densities in both hemispheres are about $110 \text{ m}^2 \text{ day sec}^{-2} \text{ rad}^{-1}$ at 1/14 day, 80 at 1/9 day, and 50 at 1/4 day. The intersection of the zonal and meridional spectral density curves occurs at a lower frequency (1/25 day) for the New Zealand

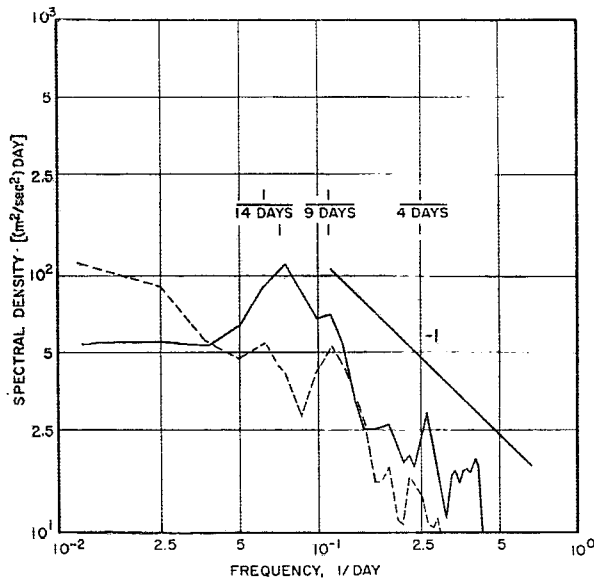


FIG. 8. Spectra of the Christchurch, New Zealand, 200-mb zonal (dashed line) and meridional (solid line) Eulerian wind for 1966. The -1 line indicates the slope of a k^{-1} exponential function. Data taken at 0000 GMT.

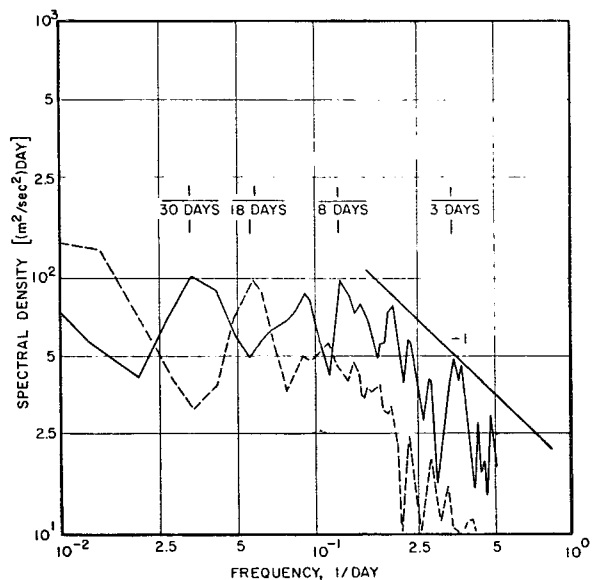


FIG. 10. Same as Fig. 8 except for Kerguelén Island (49°21'S, 70°13'E).

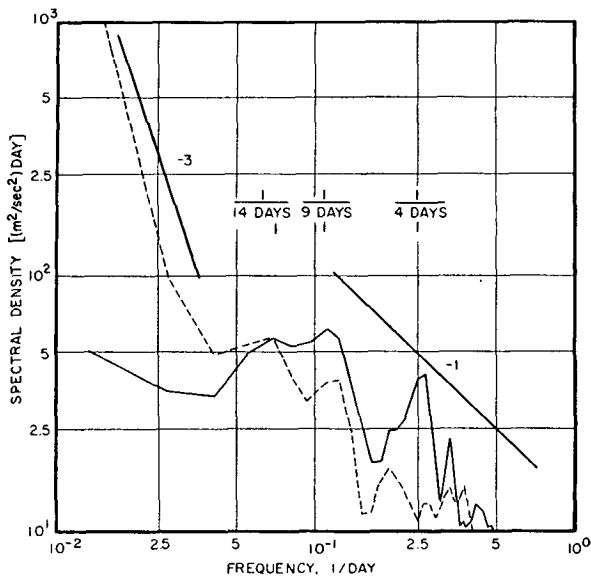


FIG. 11. Same as Fig. 9 except that the “fast Fourier” computation was used. The -1 and -3 lines indicate the slopes of k^{-1} and k^{-3} exponential functions, respectively.

stations than the frequency (1/14 day) calculated for the Northern Hemisphere station (Washington, D. C.) used by Vinnichenko. This would indicate that the anisotropy of Southern Hemisphere disturbances, with the energy in the v component exceeding that in the u component, tends to extend to longer wavelengths than is the case with Northern Hemisphere disturbances.

The density of the zonal component of the New Zealand 200-mb winds is only about one-half that found in Washington, D. C., over the synoptic scale range. Converted values for Washington and New Zealand in $m^2 \text{ day sec}^{-2} \text{ rad}^{-1}$ are shown in Table 1.

Thus, it appears that the zonal perturbation motions at planetary wave scale expressed, for instance, by jet maxima embedded in the hemispheric jet-stream belts, are stronger in the Northern than in the Southern Hemisphere. The mountain ranges of the Northern Hemisphere, especially the Rocky Mountains and the Himalayas, give rise to frequent and strong jet maxima over the eastern United States and over Japan. Quasi-inertial oscillations (Newton, 1959) may give rise to additional disturbances farther downstream. Over the Southern Hemisphere the orographic influences seem to be less effective in generating quasi-zonal jet maxima. A larger data sample, using additional stations for spectral analysis, would be needed to remove any local bias from these rather sweeping conclusions. Neverthe-

TABLE 1. Spectral densities ($m^2 \text{ day sec}^{-2} \text{ rad}^{-1}$) of the zonal components of the 200-mb winds at selected frequencies.

	1/14 day	1/9 day	1/4 day
Washington, D. C.	120	50	28
New Zealand	50	50	15

less, this preliminary study indicates that the “text-book motion” of the prevailing zonal character of the Southern Hemisphere circulation will have to be abandoned. The slope of the zonal component spectra is approximately -1 as shown in Figs. 8–10. Vinnichenko claims the same spectral slope for Northern Hemisphere data, whereas Kao (1965) finds a slope of -2 .

The spectrum of the zonal component of the Eulerian wind computed by Chiu (1960) for 200 mb for Belmar, N. J., also approximates a -1 slope with a peak density at about 1/3 day. Generally the density decreases with increasing frequency. In the range of traveling disturbances the spectrum of the meridional component for Belmar shows peak densities at 1/20 and 1/7 day, and a slope of $-5/3$. A variety of slopes was indicated at different levels at Belmar ranging from $-2/3$ at 700 mb to $-5/3$ at 300 mb and -1 at 50 mb, with an average normalized slope of -1 for the zonal component.

Spectral densities for latitudes 20, 40 and 70N were calculated for the zonal and meridional wind components at 300 mb for winter and summer by Benton and Kahn (1958) in terms of energy vs wavenumber. They found a broad peak in the power spectrum of the meridional component for 40N centered at wavenumber 6, which was interpreted as related to planetary free waves. The zonal spectral density decreased with increasing frequency except for a small peak, also at wavenumber 6. This wavenumber region corresponds to the period of about 1/14 day in the New Zealand Eulerian spectra. The ratio of the kinetic energies of the meridional to zonal wind variance from Benton’s and Kahn’s Northern Hemisphere data was found to be about 3 to 2. The data from Invercargill and Christchurch shows a ratio of meridional to zonal wind variance of about 2 to 1 at a frequency of 1/14 day. Vertical profiles of spectral densities for the Northern Hemisphere synoptic scale prepared by Vinnichenko verify that spectral densities for the 200-mb level are equal to or slightly greater than those for 10 km and 300 mb.

The spectral values in the wavenumber space for 40N (Benton and Kahn, 1958) were transferred by Vinnichenko to a log-log diagram in frequency space in units of $km^3 \text{ hr}^{-2}$ vs km^{-1} . In this presentation they appear to have a slope of -3 in the range of synoptic-scale eddies. As pointed out by Vinnichenko, the slopes of the spectra in the two representations differ markedly, and the relationship between time and space spectra can be reconciled best by means of group velocities.

The need for exercising care in comparing spectra in time and space was also brought out by Chiu and Crutcher (1966). Planck’s radiation law was used as an example for which a certain energy spectrum could have a peak at one period in one presentation and a peak at quite a different period in another presentation. Considerable difficulty follows when reconciliation is sought between spectra in the existing literature due to the several methods of presentation and varieties of spectral computational techniques and normalizations.

As an example, the Invercargill and Christchurch data were subjected to the "fast Fourier" spectral computation in addition to the standard Blackman and Tukey method shown earlier (Figs. 8 and 9). The results of this "shortcut" method are given in Figs. 11 and 12, respectively. The mid-frequency portion representing synoptic-scale disturbances retained the same approximate -1 slope and the characteristic peaks, although spectral densities at $1/14$ day were reduced substantially as compared with results from the Blackman-Tukey method (Figs. 8 and 9). The greatest difference occurred in the low-frequency end of the zonal spectrum where the spectral density was greatly increased and caused an apparent -3 slope in the low wavenumbers. This is probably due to the "bell tapering" of the first and last 10% of the data during application of the "fast Fourier" calculations and to the smoothing of the spectral estimates in the lower frequencies.

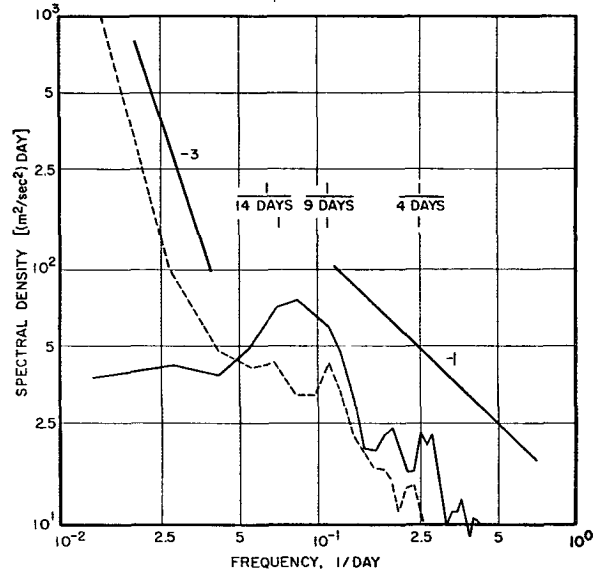


FIG. 12. Same as Fig. 8 except that the "fast Fourier" computation was used.

d. Comparison of Lagrangian and Eulerian spectra

The spectral density peak of the New Zealand Eulerian meridional wind component occurs at a lower frequency ($1/14$ day) than that of the Lagrangian relative velocity of balloon separation ($1/52$ hr). Kao (1965) found an Eulerian peak for the meridional component of the Salt Lake City 300-mb wind at about $1/8$ day and a Lagrangian peak at about $1/50$ hr. The spectral densities at the peaks are comparable for the Eulerian and Lagrangian computations in the Southern Hemisphere, in contrast to Kao's finding of about twice

the spectral density in the Eulerian velocity as compared to the Lagrangian one.

e. Eulerian cospectra

The nature of the transport of relative angular momentum is brought out in the New Zealand Eulerian zonal-meridional wind cospectra shown in Fig. 13. There is a lack of agreement between the Invercargill and Christchurch cospectra at low frequencies, but

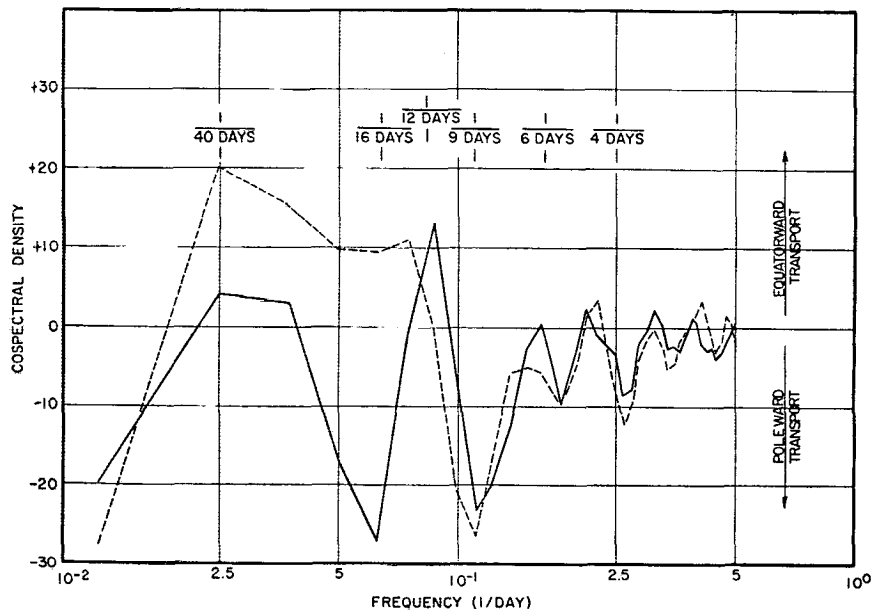


FIG. 13. Cospectra of the Christchurch (dashed line) and Invercargill (solid line) zonal-meridional 200-mb Eulerian wind components for 1966. Positive ordinate values indicate equatorward transport of relative angular momentum; negative values indicate poleward transport.

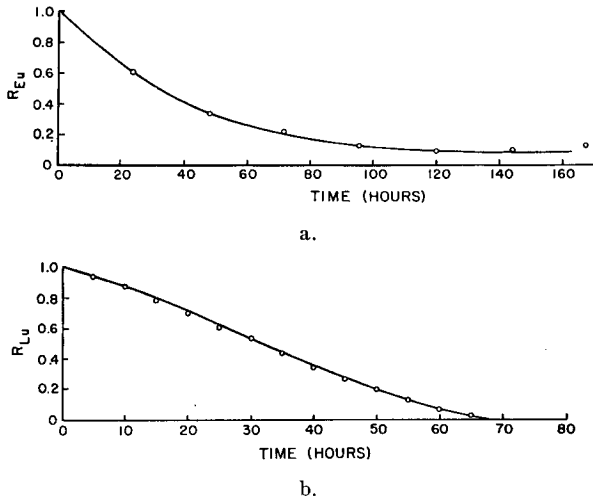


FIG. 14. Autocorrelation function of the zonal component of New Zealand 200-mb winds, a., and the GHOST balloon relative separation velocities at 200 mb, b.

very close agreement at frequencies $>1/13$ day. The disparity at low frequencies may be due to the location of Christchurch in the lee of the New Zealand Alps, whereas Invercargill lies on the southern plains of South Island.

Poleward transport of momentum is indicated at frequencies near $1/16$ day for Invercargill and at frequencies $>1/10$ day at both New Zealand stations at 200 mb. The equatorward transport at frequencies from $1/40$ to $1/12$ day at Christchurch is probably due to the preferred location of an orogenic lee trough east of the Southern Alps which rise to elevations of 3 km.

Chiu and Crutcher (1966) found that the major transport of angular momentum for North American stations was contributed by oscillations of frequency $<1/5$ day, and that spectra were quite similar for all levels at any given station. Tatoosh Island, perhaps the most suitable of the North American stations for comparison with Invercargill, showed good agreement with poleward transport at 200 mb at frequencies from $1/20$ to $1/4$ day.

Obasi (1963) found the transport of relative angular momentum in the Southern Hemisphere to be poleward at 45S in the transient eddies and equatorward, but less pronounced, in standing eddies. The poleward transport indicated during summer and winter in the planetary waves traversed by the GHOST balloons (Fig. 7) corresponds to the transport at frequencies from $1/25$ to $1/6$ day indicated in the Invercargill cospectrum of Fig. 13.

4. Macroscale eddy diffusion

Kao (1962) showed that the autocorrelation coefficients $R_u(\tau)$ and $R_v(\tau)$ computed from a lag-products

could be represented as

$$\left. \begin{aligned} R_u(\tau) &= \exp(-\epsilon_u \tau) \\ R_v(\tau) &= G \left(\frac{\sin \Delta \omega \tau}{\Delta \omega \tau} \right) \cos \bar{\omega} \tau + H \exp(-\epsilon_v \tau) \end{aligned} \right\} \quad (4)$$

where

$$\left. \begin{aligned} G &= \frac{A^2}{A^2 + 2v_r^2} \\ H &= \frac{2v_r^2}{A^2 + 2v_r^2} \end{aligned} \right\} \quad (5)$$

and A is planetary wave amplitude, v_r velocity of the dispersing particles in the cluster (measured relative to the center of gravity), ϵ_u and ϵ_v are proportional to the integral time scale, and

$$I_u = \int_0^\infty R_u(\tau) d\tau. \quad (6)$$

An analogous equation holds for I_v . Finally

$$\left. \begin{aligned} I_u &= \frac{1}{\epsilon_u} \\ I_v &= \frac{H}{\epsilon_v} \end{aligned} \right\} \quad (7)$$

Figs. 14a and b show the autocorrelation functions of the zonal components of the New Zealand 200-mb Eulerian winds and the GHOST balloon relative separation velocities, respectively. An analysis of the curves using (4) yields values of $\epsilon_{Eu} = 0.61 \times 10^{-5} \text{ sec}^{-1}$ for the Eulerian system and $\epsilon_{Lu} = 1.02 \times 10^{-5} \text{ sec}^{-1}$ for the Lagrangian system in the Southern Hemisphere. Kao (1965) found that $\epsilon_{Eu} = 0.94 \times 10^{-5} \text{ sec}^{-1}$ and $\epsilon_{Lu} = 1.58 \times 10^{-5} \text{ sec}^{-1}$ at 300 mb in the Northern Hemisphere.

The autocorrelation functions of the meridional components are displayed in Fig. 15a for the New Zealand winds and in Fig. 15b for the GHOST balloon relative separation velocities. The value of H , computed from (5), is 0.32 in the Southern Hemisphere at 200 mb as compared to 0.30 in the Northern Hemisphere at 300 mb (Kao, 1965).

The transformation between Lagrangian and Eulerian spectral energies on the planetary wave scale (Kao, 1965) has been proposed as

$$R_L(\eta) = R_E(\tau), \quad (8)$$

where $\eta = \beta^* \tau$.

The ratio β^* of the Lagrangian to Eulerian integral time scales can be shown to be.

$$\beta^* = \frac{I_{Lv}; \epsilon_{Eu}}{I_{Ev}; \epsilon_{Lu}}. \quad (9)$$

For the Southern Hemisphere winds analyzed here, the ratio β^* is 0.60.

The zonal and meridional components of the planetary wave scale eddy diffusivity can be expressed as

$$K_x = \frac{\overline{u'L^2}}{\epsilon L u}, \tag{10}$$

$$K_y = \frac{H_L \overline{v'L^2}}{\epsilon L v}, \tag{11}$$

where $u'L^2$ and $v'L^2$ are the mean variances of the zonal and meridional Lagrangian relative velocity components of a dispersing particle cluster.

The macroscale eddy diffusivity components computed for summer, winter and annual means using GHOST balloon data are listed in Table 2. Also listed are values calculated by Kao and Bullock (1964), Kao (1965), and Kao (1969), computed with $\overline{u'L^2} = \overline{v'L^2} = 3.24 \times 10^6 \text{ cm}^2 \text{ sec}^{-2}$. The GHOST data yielded $\overline{u'L^2} = 0.81 \times 10^6 \text{ cm}^2 \text{ sec}^{-2}$ and $\overline{v'L^2} = 0.54 \times 10^6 \text{ cm}^2 \text{ sec}^{-2}$ for the annual mean. These differences in the variances of the velocity components are the main reason why the annual mean values of K_x and K_y turn out to be smaller in the Southern Hemisphere than those computed by Kao (1965, 1969) for the Northern Hemisphere.

Kao and Bullock (1964) used 500-mb geostrophic trajectories, obtaining substantially lower values of K_x and K_y than Kao (1965), who used 300-mb constant pressure balloon flights as a data source (see Angell, 1960) and Kao (1969) who used 200-mb geostrophic trajectories. The lower values at 500 mb might be expected because of generally smaller wind velocities there.

The data for the Southern Hemisphere presented in Table 2 reflect the increase in the spectral densities of the meridional component from winter to summer mentioned earlier. Even though the cyclone waves in the

TABLE 2. Macroscale eddy diffusivity components ($10^6 \text{ m}^2 \text{ sec}^{-1}$).

	K_x	K_y	K_x/K_y
Southern Hemisphere			
Summer	5.03	2.11	2.38
Winter	10.9	1.26	8.66
Annual	7.88	1.69	4.67
Northern Hemisphere			
Summer*	4.05	1.16	3.49
Winter*	6.30	2.90	2.17
Annual*	5.90	2.30	2.56
Annual**	20.5	6.15	3.33
Annual***	23.6	5.8	4.07

* From Kao and Bullock (1964).
 ** From Kao (1965).
 *** From Kao (1969).

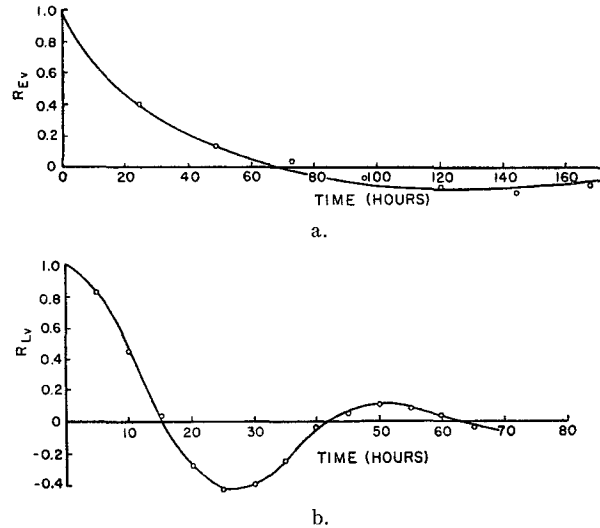


FIG. 15. Same as Fig. 14 except for the meridional component.

Southern Hemisphere are strongly anisotropic in favor of the meridional component of motion, the interplay of all frequencies $> 1/7$ day greatly enhances the zonal dispersion during the Southern Hemisphere winter (and also in the annual mean). The spline function smoothing which has been applied to the GHOST data may have reduced somewhat the high-frequency contribution to the variances which entered into the estimates of K_x and K_y .

5. Conclusions

GHOST balloon experiments conducted in the Southern Hemisphere yielded valuable data on atmospheric motions in a quasi-Lagrangian coordinate system. It was shown that such Lagrangian tracers are capable of portraying the phase velocities of cyclone and planetary waves; however, they are not adequate in depicting group velocity effects. Spectrum analysis of the relative motion components of pairs of GHOST balloons measured during the Southern Hemisphere summer and winter revealed interesting differences of motion patterns in the two hemispheres.

The spectra of the v component of the relative velocity of balloon pairs reveal a peak at a frequency near $1/52 \text{ hr}$, and a slope at higher frequencies suggesting a proportionality of the spectral density to k^{-3} . The high-frequency end of the balloon spectra is strongly influenced, however, by the spline function which was applied for the purposes of smoothing and of interpolating hourly balloon position points. Nevertheless, it appears significant that the energy in the v component exceeds that in the u component at this peak frequency of $1/52 \text{ hr}$ by a ratio of 10 to 1 (8 to 1 if the spectra are normalized) in the Southern Hemisphere, whereas in the Northern Hemisphere this ratio seems to lie near 3 to 1. In corroboration of this statement, cyclonic

cloud vortices, on the average, seem to be stretched latitudinally more in the Southern Hemisphere than in the Northern.

Spectral densities of the meridional component of Eulerian winds measured at Invercargill and Christchurch, New Zealand, and Kerguelen Island were similar to those reported by Vinnichecko for Northern Hemisphere stations. In the New Zealand spectra, however, the energy in the v component of perturbation motions appears to exceed that in the u component to lower frequencies (1/25 day) than in the Northern Hemisphere (1/14 day). The zonal component of the New Zealand data shows less energy at planetary- and cyclone-wave frequencies than is evident from Washington, D. C., data. This may be due to a relative lack of orographically generated jet maxima in the Southern Hemisphere, superimposed upon the hemispheric (zonal) jet-stream bands.

The ratio of Lagrangian to Eulerian spectral densities is significantly larger than 1 in the Southern Hemisphere at low frequencies and, according to Kao (1965), is 0.33 in the Northern Hemisphere.

From the sparse GHOST balloon data presently available from the Southern Hemisphere, it appears that the eddy diffusivity coefficients at jet stream levels are smaller there in the annual average than over the Northern Hemisphere, with the exception of the summer season. The ratio of K_x/K_y is larger in the Southern than in the Northern Hemisphere, again with the exception of summer. Since the energy contained in the v component of cyclone waves shows the opposite hemispheric pattern we have to conclude that the velocity variances caused by long planetary waves are the main cause of the "zonal" character of the Southern Hemisphere large-scale eddy diffusivity. The far-spread notion that motions in the Southern Hemisphere are predominantly zonal in comparison with Northern Hemisphere conditions is certainly not valid on the scale of traveling cyclones.

Acknowledgments. The authors are indebted to Mr. Samuel B. Solot for making the GHOST balloon data available and for explaining certain aspects of the treatment of that data. The initial evaluation of the GHOST data was performed by Mr. Dennis Walts. Computer programs were developed and run by Mr. T. K. Kochneff; Mrs. Sandra Olson typed the manuscript.

REFERENCES

- Angell, J. K., 1960: An analysis of operational 300 mb transosonde flights from Japan in 1957-58. *J. Meteor.*, **17**, 20-35.
- Batchelor, K. G., 1950: Application of the similarity theory of turbulence to atmospheric diffusion. *Quart. J. Roy. Meteor. Soc.*, **17**, 133-146.
- Benton, G. S., and A. B. Kahn, 1958: Spectra of large-scale atmospheric flow at 300 millibars. *J. Meteor.*, **15**, 401-410.
- Blackman, R. B., and J. W. Tukey, 1958: *The Measurement of Power Spectra from the Point of View of Communications Engineering*. New York, Dover Publ., 190 pp.
- Chiu, Wan-cheng, 1960: The wind and temperature spectra of the upper troposphere and lower stratosphere over North America. *J. Meteor.*, **17**, 64-77.
- , and H. L. Crutcher, 1966: The spectrums of angular momentum transfer in the atmosphere. *J. Geophys. Res.*, **71**, 1017-1032.
- Gibbs, W. J., 1952: Notes on the mean jet stream over Australia. *J. Meteor.*, **9**, 279-284.
- Hutchings, J. W., 1950: A meridional atmospheric cross-section for an oceanic region. *J. Meteor.*, **7**, 94-100.
- Jenkinson, A. F., 1955: Average vector wind distribution of the upper air in temperate and tropical latitudes. *Meteor. Mag.*, **84**, 140-147.
- Kao, S.-K., 1962: Large-scale turbulent diffusion in a rotating fluid with applications to the atmosphere. *J. Geophys. Res.*, **67**, 2347-2459.
- , 1965: Some aspects of the large-scale turbulence and diffusion in the atmosphere. *Quart. J. Roy. Meteor. Soc.*, **91**, 10-17.
- , 1969: Large-scale dispersion of clusters of particles in the atmosphere. II. Stratosphere. *J. Atmos. Sci.*, **26**, 734-740.
- , and A. A. al-Gain, 1968: Large-scale dispersion of clusters of particles in the atmosphere. *J. Atmos. Sci.*, **25**, 214-221.
- , and W. S. Bullock, 1964: Lagrangian and Eulerian correlations and energy spectra of geostrophic velocities. *Quart. J. Roy. Meteor. Soc.*, **90**, 166-174.
- Mantis, H. T., 1963: The structure of winds of the upper troposphere at mesoscale. *J. Atmos. Sci.*, **20**, 94-104.
- Namias, J., 1947: Physical nature of some fluctuations in the speed of the zonal circulations. *J. Meteor.*, **4**, 125-133.
- Newton, C. W., 1959: Axial velocity streaks in the jet stream: Ageostrophic "inertial" oscillations. *J. Meteor.*, **16**, 638-645.
- Obasi, G. O. P., 1963: Poleward flux of astmopheric angular momentum in the Southern Hemisphere. *J. Atmos. Sci.*, **20**, 516-528.
- Petterssen, S., 1956: *Weather Analysis and Forecasting*, Vol. 1, *Motion and Motion System*. New York, McGraw-Hill, 428 pp.
- Radok, U., and R. H. Clarke, 1958: Some features of the subtropical jet stream. *Beitr. Phys. Atmos.*, **31**, 89-108.
- Reiter, E. R., 1958: Die Verwendung von Kontinuitätsdiagrammen in der nordalpinen Wetterprognose. *Arch. Meteor. Geophys. Bioklim.*, **A10**, 161-177.
- Solot, S. B., 1968: GHOST balloon data, Vols. I-XI. NCAR Tech. Notes, NCAR TN-34.
- Taljaard, J. J., 1967: Development, distribution and movement of cyclones and anticyclones in the Southern Hemisphere during the IGY. *J. Appl. Meteor.*, **6**, 973-987.
- van Loon, H., 1964: Mid-season average zonal winds at sea level and at 500 mb south of 25 degrees south and a brief comparison with the Northern Hemisphere. *J. Appl. Meteor.*, **3**, 554-563.
- , 1965: A climatological study of the atmospheric circulation in the Southern Hemisphere during the IGY, Part I: 1 July 1957-31 March 1958. *J. Appl. Meteor.*, **4**, 479-491.